Cultural Heritage and Science
https://dergipark.org.tr/en/pub/cuhes
e-ISSN 2757-9050

Mineralogical and geochemical characterisation of granite columns from the ancient city of Tyana (Niğde, Türkiye) and implications for their origin

Hacer Bilgilioğlu[*1]

[1]*Aksaray University, Faculty of Engineering, Department of Geological Engineering, Aksaray, Türkiye*

Cite this study: Bilgilioglu, H. (2025). Mineralogical and geochemical characterisation of granite columns from the ancient city of Tyana (Niğde, Türkiye) and implications for their origin. Cultural Heritage and Science, 6 (1), 53-65.

https://doi.org/10.58598/cuhes.1629100

Keywords
Granite columns
Petrography
Geochemistry
Ancient city of Tyana

Research Article

Received:29.01.2025
Revised:17.04.2025
Accepted:30.04.2025
Published:01.06.2025

Abstract

In this article, the mineralogical, petrographic and geochemical properties of the granite columns, which are significant architectural elements in the ancient city of Tyana in the Cappadocia region, are documented and their origins are inferred. Tyana granite columns have porphyro-aphanitic texture and are characterized by mega crystals. The main mineral assemblage in the the granite columns consists of K-feldspar, quartz, plagioclase, biotite, amphibole and accessoy titanite, zircon and opaque minerals. XRD analysis supports the primary mineral assemblage. CRS (Confocal Raman Spectroskopy) studies also revealed that the plagioclase is andesine and amphibolite is actinolite in composition. In addition, geochemical analyses revealed that the granite columns are calc-alkali and granodiorite in composition. In the tectonic evaluation, the granite samples are located in the area of volcanic arc granitoids. According to all analysis results, the Tyana granite columns are compatible with the Horoz granitoids. All the above features will be an important step for the conservation and restoration of future ancient structures.

1. Introduction

Natural stone is one of the main materials used in ancient buildings due to its durability and aesthetic properties. Natural stones such as marble, limestone, and granite were favored in public spaces such as temples and colonnades, especially in monumental buildings [1]. The natural stones used in historic buildings provided aesthetics and functionality, while simultaneously allowing them to resist environmental conditions. Identifying the sources of natural stone also plays an important role in the conservation and restoration of built heritage and monuments [2–8]. Among these natural stones, granite is an important building material with excellent physical and chemical durability and is widely used for various purposes, especially obelisks. Granite columns used in ancient architecture were not only a decorative element but also formed an important structural component that ensured the strength of built structures. Granite has played a critical role in the preservation of many archaeological structures due to its long-term resistance to abrasion, climatic factors, and biological degradation [3, 9, 10].

Granitic rocks are some of the most important raw materials widely used throughout the Egyptian, Greek, Roman, Byzantine, and Ottoman eras for various purposes, including for obelisks, statues, temples, baths, sarcophagi, columns, and decorative building materials. Today, as in the past, many people (except geologists) use the term “granite” to refer to fully crystalline rocks of different colors. For this reason, many granitic rocks, especially those used in historic buildings, have been classified as granite without adequate petrographic research; however, geoscientists use the term “granite” without microscopic examination. Granite is composed primarily of K-feldspar (orthoclase and microcline), plagioclase (albite, oligoclase, and andesine), quartz, biotite, and amphibole. In recent years, multiple analytical approaches have been applied to identify the scientific characteristics and origins of granitic rocks of

uncertain provenance [11–19]. Studying the mineralogical, petrographic, and chemical properties of granite columns provides important insights into the sources, processing techniques, and transportation methods of the stone used in the periods when these structures were built.

The granite columns selected as the subject of this study are situated in the ancient city of Tyana. The ancient city of Tyana is located in the Cappadocia region in Turkey and was considered an essential trade center during the Roman Empire. The granite columns in this region stand are an important architectural feature in ancient buildings. Despite various studies on granite columns in many ancient city to date [20–22] the provenance of the Tyana granites remains poorly understood. To address this issue, in this article Tyana granite columns were analyzed in detail using optical microscopy, X-ray diffraction (XRD), X-ray fluorescence (XRF), and confocal Raman spectroscopy (CRS) techniques to reveal their mineralogical and petrographic properties, crystallographic structures, and chemical compositions. Mineralogical and petrographic investigations of the Tyana granite columns have indicated their potential relationship with the region's Horoz Granitoid and Üçkapılı Granite rocks. These comparisons can provide important clues regarding the origin of the columns. Here, the igneous processes affecting the formation of the granite columns were interpreted and compared with potential granite sources in the region. Understanding this relationship will help elucidate the commercial and architectural context of Tyana.

2. History of Tyana Ancient City

The ancient city of Tyana, an important settlement during the Hittite, Roman, and Byzantine eras, was built in the town of Kemerhisar in Niğde (Figure 1). Tyana, which is approximately 23 km from Niğde city center, is located approximately 5 km to the southeast of Bor district. In ancient times, its strategic location in the Cappadocia Region, connecting Cilicia and Cappadocia, led to the conquest of the city multiple times by different civilizations. Throughout history, Tyana was variously referred to as "Tuwanuwa" during the Hittite period, "Tuwana" during the Late Hittite period, "Dana" during the Persian and Hellenistic periods, "Tyana" during the Roman Empire, "Kilisehisar" during the Ottoman Empire, and "Kemerhisar" during the Republic of Turkey. During the Christian era, it was also known as "pilgrims' road (Hacıyolu)" because it was used by pilgrims going to Jerusalem due to its location on the pilgrimage route [8, 23–25].

According to Strabo, Tyana was a prominent settlement due to its fertile and flat lands, strong fortifications, and strategic location. Strabo also noted that Tyana was named Eusebeia, near the Taurus Mountains, to distinguish it from Kaisareia (Mazaka/Kayseri). After their liberation from Seleucid rule, two important cities in Cappadocia—Kaisareia and Tyana—were rebuilt by Ariarathes V Eusebes Philopator. Tyana was named "Eusebeia" in honor of its founder and is thought to be connected to the rites held for Zeus in the temple of Asbamaios near the sacred lake [23, 26, 27]. Septimius Severus' admiration for Apollonius of Tyana is recognized as one of the primary factors that bolstered the city's importance. In later periods, his son Caracalla also admired Apollonius greatly. During the Severus dynasty, various construction works were conducted in the city; structures such as aqueducts, the Roman Pool, a temple dedicated to Zeus Asbamaios, the Roman Baths, and the Heroon were built. Tyana, which gained importance during the empire of Caracalla (211–217 AD), was elevated to the status of "Colonia" and named Antoniana Colonia Tyana [28–30]. It is thought that Caracalla's declaration of Tyana as a Colonia was due to his desire to use this region as a base for his campaigns to the east by taking advantage of the city's strategic location extending to Syria [28]. In addition, Caracalla and his mother Julia Domna attached great importance to Tyana and carried out extensive reconstruction in the city. The aqueducts to the south of the city were also built during the reign of Caracalla and were constructed with a complex hydraulic system to bring water to the city from the hills. These aqueducts were designed to supply water to all residences in the city [24].

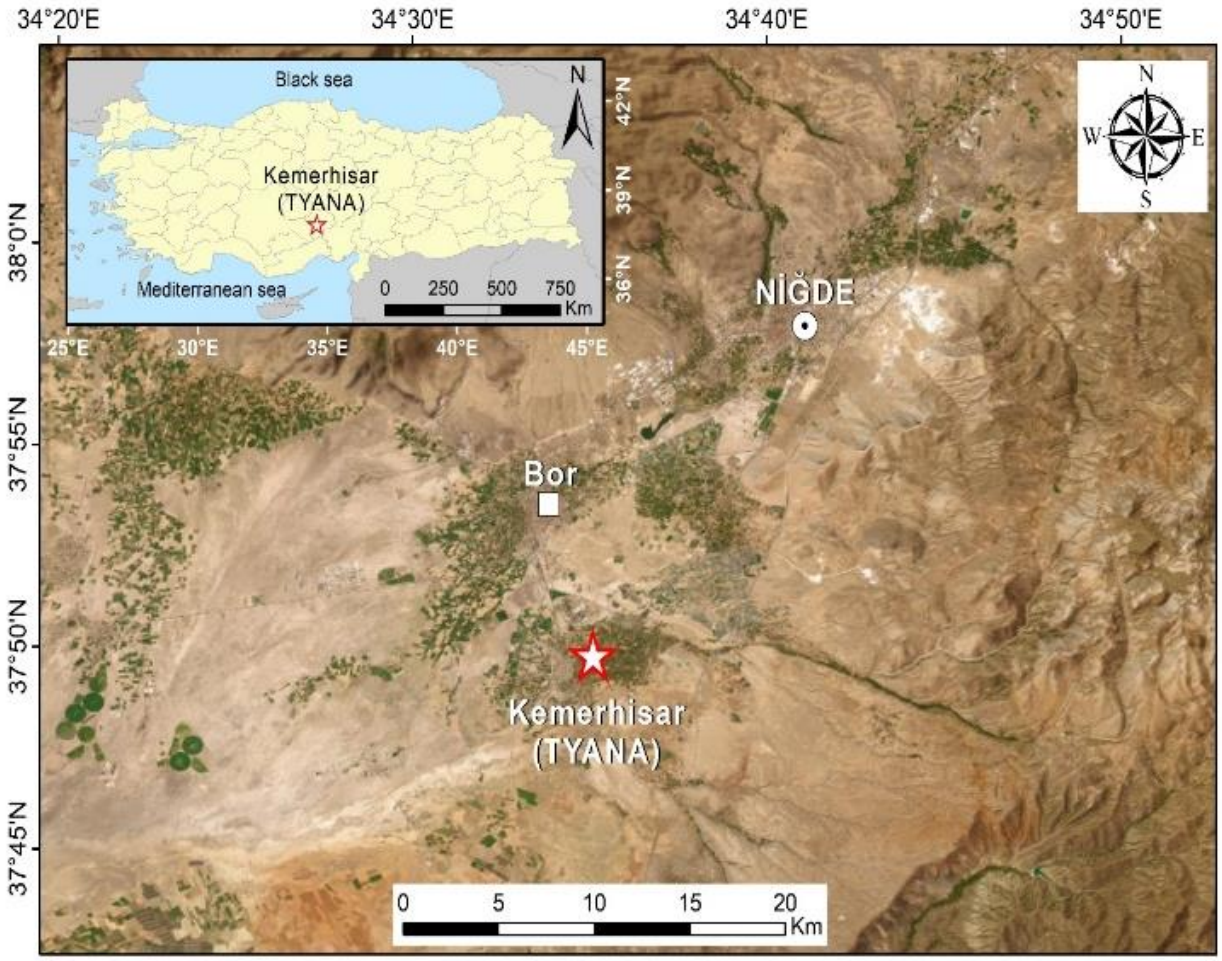

Figure 1. Location of study area

3. Geological Settings

Tyana is located in the Central Anatolia Region, 5 km from Bor district of Niğde province. The Niğde region is adjoined by the Aladağlar Mountains to the southeast and the Bolkar Mountains to the south. This region represents the area in which the Taurides and Anatolides meet [31]. The Niğde Massif is located to the southeast of Niğde and forms the southernmost part of the Central Anatolian Massif [31, 32]. The metamorphic rocks of the Niğde Massif form part of the Niğde Group and are divided into the Gümüşler, Kaleboynu, and Aşıgediği formations based on their lithology and are cut by the Üçkapılı granodiorite [32, 33]. The Niğde Group rocks, which underlie the study area, are medium–high-grade Paleozoic metamorphic rocks and form the southern part of the Central Anatolian Crystalline Complex. These metamorphic rocks are overlain by Upper Cretaceous ophiolites [32, 34].

In addition to the Gökbez formation and Kızılkaya ignimbrites in the Kemerhisar region, the Horoz Granitoid is an igneous unit that has contributed significantly to the geological evolution of the region [35–37].

The Horoz Granitoid is an intrusive rock belonging to the Central Anatolian Igneous Complex with similar petrographic and geochemical characteristics to the Üçkapılı Granodiorite in the southeast of the Niğde Massif. Similar to the Üçkapılı Granodiorite, which cuts Paleozoic Niğde Group metamorphic rocks, the Horoz Granitoid has intruded the area's variably metamorphosed metamorphic rocks. In the Kemerhisar region where the study area is located, the Kızılkaya ignimbrites and Gökbez formation unconformably overlie Niğde Group metamorphic rocks [38]. The Miocene–Pliocene Gökbez Formation occurs in large areas around the ancient city of Tyana and comprises marl–limestone–mudstone deposits with bituminous levels and travertine interlayers in the upper parts of the formation. The thickness of the Gökbez formation varies in the range of 50–150 m [33]. The travertine deposits in the upper part of the Gökbez formation, which is located close to the study area and thus a suitable source of blocks, were used in the construction of the Tyana aqueducts. The Gökbez formation consists of sediments deposited in a lake environment with transport from north to south, and during its deposition, it received clastic input from the Niğde Group metamorphic rocks and Havuzlu ignimbrites [8, 39, 40].

The primary aim of this study is to investigate the mineralogical, petrographic, and geochemical characteristics of granite columns located in the ancient city of Tyana in order to determine their provenance and evaluate their potential connections with nearby granitoid formations, particularly the Horoz Granitoid and Üçkapılı Granite. By employing a combination of analytical techniques—including optical microscopy, X-ray diffraction (XRD), X-ray fluorescence (XRF), and

confocal Raman spectroscopy (CRS)—this research seeks to clarify the geological origin, material properties, and historical usage of the granite columns.

4. Materials and methods

Based on the study's objectives, the granite column samples were first visually examined on-site, and their macroscopic characteristics were determined. It is believed that the studied granite columns were building materials used in courtyards, columns, and the porticoes of buildings. The Tyana granite columns were then characterized using the steps detailed below. Thin sections were prepared as a basic analysis method to examine the mineralogical and petrographic properties of the samples in detail, i.e., their mineral associations, grain sizes, and textures.

XRD spectroscopy is a powerful analytical technique that can be used to study the crystal structural properties of a substance. This technique allows the arrangement of atoms in the internal structure of materials to be determined and reveals the composition of minerals qualitatively. These analyses were performed with an Inel Equinox 1000 instrument using a Co tube with a wavelength of 1.788970 Å. The XRD analyses were performed using a Panalytical X'Pert Powder device at the Department of Mineral Analysis and Technology of the General Directorate of Mineral Research and Exploration. This device was used to examine the crystal structure of the granite columns, with the results providing important insights into the detailed mineralogical characteristics of the rocks.

For further mineralogical characterization, selected granite column samples were analyzed using the CRS technique. The CRS analyses were performed on polished thin sections using a Jobin Yvon (Horiba) LabRAM-800HR confocal Raman spectrometer at the Department of Geological Engineering, Ankara University. This instrument is equipped with a notch filter-based Raman microscope system, an Olympus BX41 optical microscope, a grating with 1800 grooves per mm, and a Peltier-cooled CCD detector. The Raman spectroscopy measurements were performed in the spectral range 100–4000 cm^{-1} with a resolution of 2 cm^{-1} using a He–Ne laser with a wavelength of 633 nm. Repeat measurements were obtained using the highest magnification to improve the signal-to-noise ratio, thus resulting in clearer spectra.

The main oxide and trace element compositions of the samples were analyzed via XRF spectroscopy. The XRF analyses were performed with a Panalytical Axios Max brand wavelength-dispersive XRF (WD-XRF) device in the Geochemical Analysis Laboratory of Aksaray University Application and Research Center Laboratory. The samples to be analyzed were first crushed with crusher devices and then pulverized to a size of approximately 20 microns in ball mills. The obtained powder samples were mixed with a binder material and pressed into pellets under a pressure of 12 bars. Major and trace element analyses were then performed on the prepared pellets using the WD-XRF technique.

5. Results

5.1 Mineralogy and Petrography

The fresh surfaces of the Tyana granite columns are grayish in color and show a porphyrophaneritic texture upon macroscopic examination (Figure 2a). Plagioclase, quartz, and mafic minerals can be visually identified in hand specimens of the granitic column (Figure 2b, c). Mafic minerals (biotite and amphibole) with black color and glassy luster were observed. In addition, mafic enclaves ranging in size from 5 to 10 cm, darker than the bedrock, are observed in the granite columns (Figure 2d). The granite columns are petrographically granodioritic in composition and exhibit a holocrystalline hypidiomorphic granular texture. The primary mineral assemblage comprises K-feldspar, quartz, plagioclase, mafic minerals (biotite and amphibole), and to a lesser extent titanite, zircon, and opaque minerals.

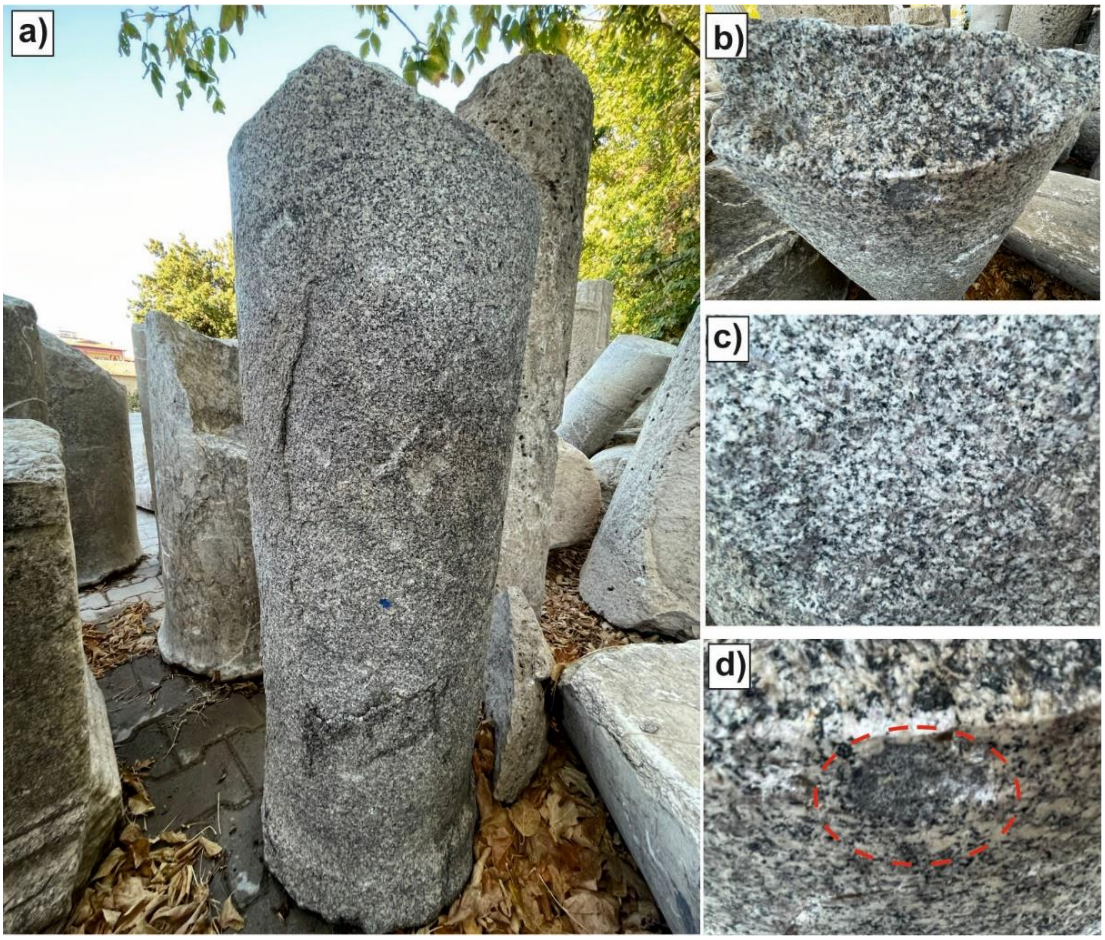

Figure 2. a) Tyana granite column b) close-up view of granite column c) granite column sample showing porphyro-phaneritic texture d) enclavs in granite columns

The observed K-feldspars typically have an orthoclase composition and occur as euhedral crystals with prismatic forms. Within the large orthoclase crystals, there are inclusions of plagioclase, quartz, and biotite interpreted as a poikilitic texture. Plagioclase occurs as subhedral to euhedral crystals, with Carlsbad twinning commonly observed in albite (Figure 3a). The plagioclases weathered to sericite and clay minerals have a slightly turbid appearance. The quartz minerals in the thin sections generally show xenomorphic crystal forms. The biotite minerals exhibit strong pleochroism ranging from light yellow to dark brown. Some biotite minerals have undergone oxidation to iron oxides. Amphibole minerals are short prismatic and subhedral crystals, with strong pleochroism ranging from light yellow-green to dark green (Figure 3b,c,d). The sphene (titanite) is characterized by development of rhombohedral crystals distinguished by sharp edges.

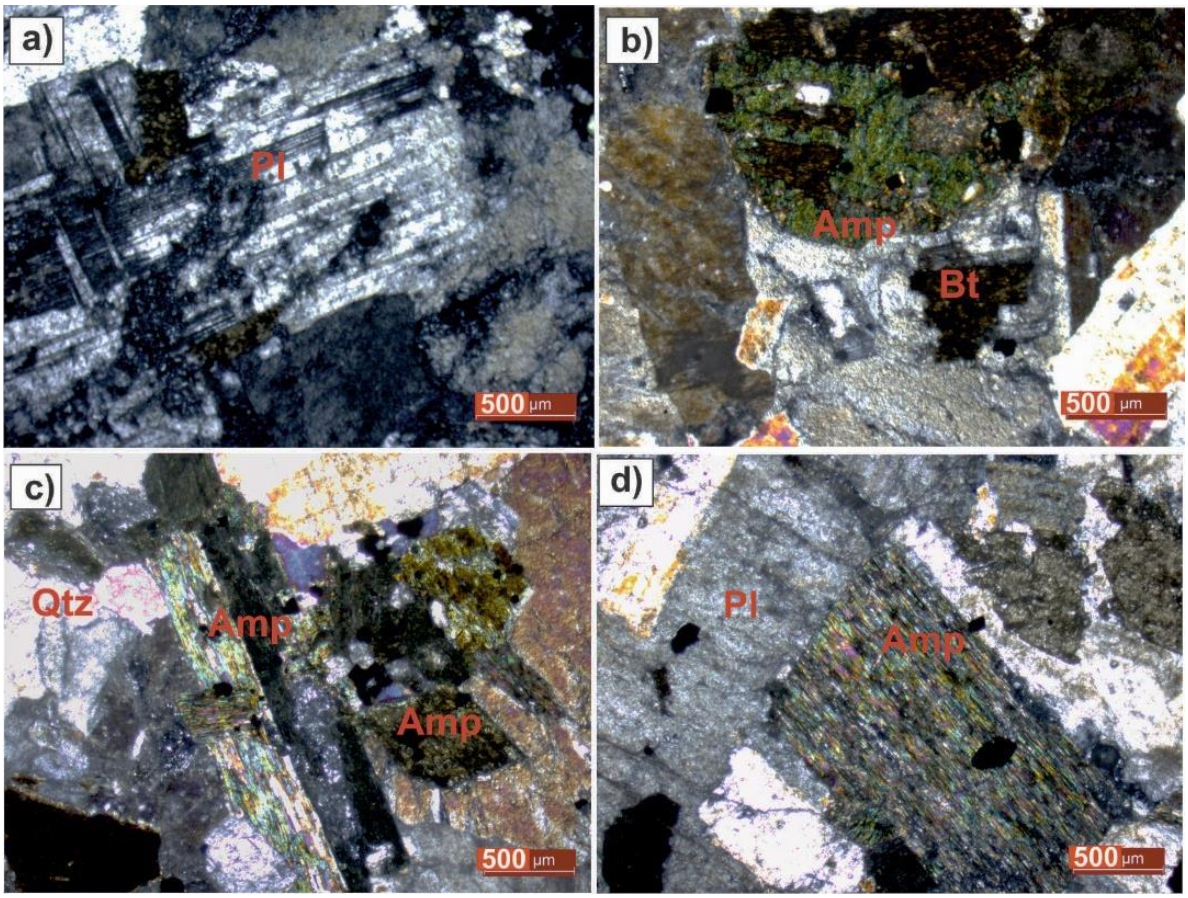

Figure 3. Optical microscope images of Tyana granite column samples a) Plagioclase showing albite polysynthetic twinning b) Amphibole and biotite minerals c) Euhedral and subhedral amphibole minerals d) Altered plagioclase and amphibole minerals (Qtz: quartz, Pl: plagioclase, Amp: amphibole, Bt: biotite)

XRD analysis was performed to determine the main mineral phases in the Tyana granite column samples in addition to the above optical microscopy analyses. The XRD analysis confirmed the presence of major mineral phases including plagioclase, quartz, K-feldspar, biotite, amphibole and sphene, consistent with the observations from optical microscopy (Figure 4).

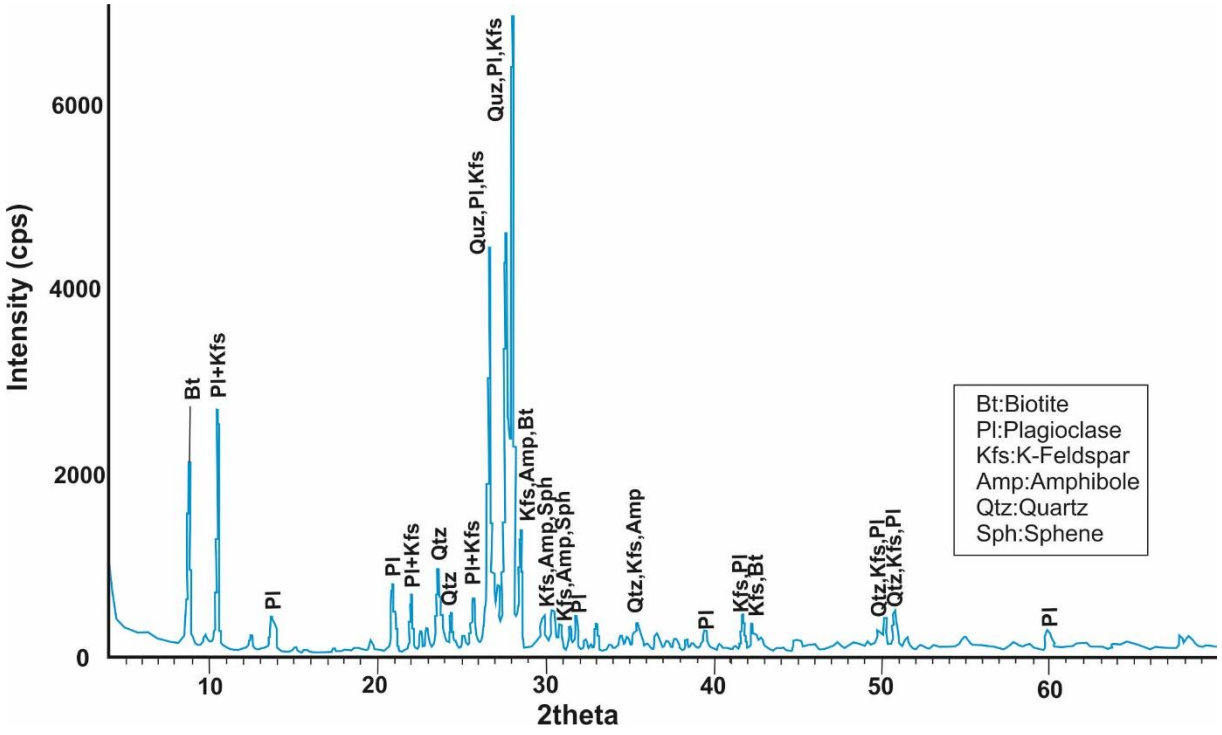

Figure 4. XRD graph of Tyana granite columns

5.2 Confocal Raman Spectroscopy (CRS)

The essence of Raman spectroscopy involves measuring a scattered beam produced by the irradiation of a powerful laser source in the visible or near-infrared wavelength region, which is used to illuminate a sample [2]. The difference in the wavelength of the scattered beam relative to the wavelength of the incident beam interacting with the molecule is referred to as a Raman shift. The Raman shift values of minerals act as "fingerprints" and can be used to effectively distinguish between minerals [41].

To determine the mineral characteristics of the Tyana granite column samples, CRS analyses were performed for plagioclase, amphibole, biotite, and quartz minerals. The characteristic peaks for biotite minerals are vibrations due to Mg-O and Fe-O bonds at 180–200 cm^{-1}, Si-O-Si vibrations at 270–300 cm^{-1}, Al-O and Fe-O vibrations at 680–700 cm^{-1}, and Si-O vibrations at 950–1100 cm^{-1}. The biotite mineral in the granite column samples shows a characteristic Raman spectrum, with the strongest peak at 189.46 cm^{-1} corresponding to Fe-O bonds. This supports the formation of ferro-biotite. (Figure 5a).

The CRS measurements identified the amphibolite type as actinolite. The characteristic Raman peaks for actinolite are typically associated with Si-O-Si tensile vibrations, corresponding to a strong peak in the 670–680 cm^{-1} range. These spectral features are distinctive features that allow the identification of actinolite-type amphiboles in Raman analysis (Figure 5b).

Strong peaks were detected in the CRS analysis of the plagioclase minerals, and the plagioclase species was identified as andesine (Figure 5c). The strongest peak corresponding to andesine was observed at 512.65 cm^{-1}. The prominent peaks in the Raman spectrum of the andesine-type plagioclase are Si-O-Si vibrations at 480–510 cm^{-1}, Al-O-Si vibrations at 500–520 cm^{-1}, and Si-O vibrations at 950–1050 cm^{-1}. These peaks may differ between andesine and other plagioclase species, and the spectrum may exhibit slight variations. The 480–510 cm^{-1} band is considered the most characteristic Raman peak for plagioclase minerals.

Quartz (SiO_2) exhibits highly distinct and strong peaks in CRS analysis. The most characteristic peak in the Raman spectrum of quartz is usually located at a wave number of 464 cm^{-1}. This is consistent with the results presented here, where the quartz measured in the samples shows a peak at 464.00 cm^{-1} (Figure 5d).

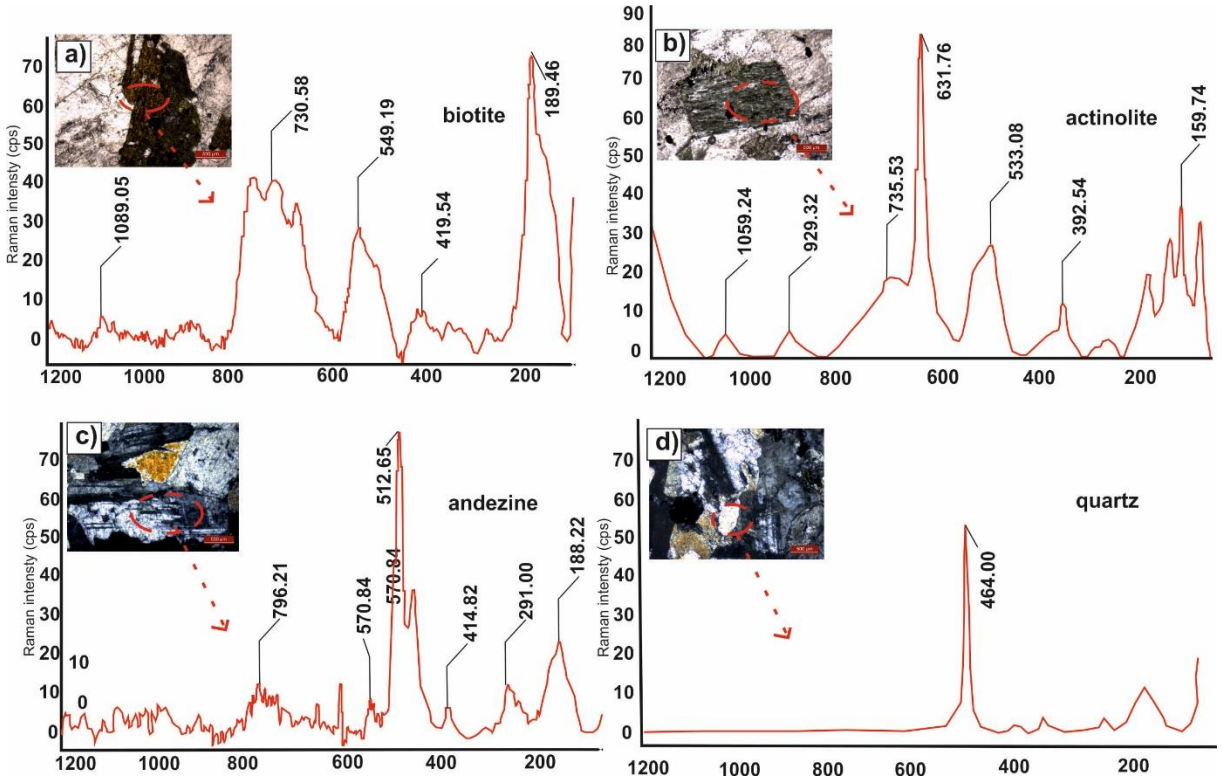

Figure 5. Point analysis results of Raman spectra of Tyana granite columns on different minerals

5.3 Geochemistry

In this study, the geochemical properties of granite columns from the ancient city of Tyana were compared with those of the Horoz Granitoid, and Üçkapılı Granitoid. The Horoz granitoid has two members, granodiorite and granite. The geochemical data for the Horoz Granite and Granodiorite were taken from [38] while the data for the Üçkapılı Granitoid were taken from [42]. These comparisons provide important constraints on the potential source region and origin of the columns and a better understanding of the connection between the granite columns at Tyana and the surrounding granitoids. The main oxide and trace element compositions of the samples belonging to the Tyana granite columns, the average main oxide and trace element compositions of the Üçkapılı Granitoid and Horoz granotid are listed in Table 1.

Table 1. Major oxide (wt.%) and trace (ppm) element analyses of Tyana granite columns, Üçkapılı granitoid (data taken from [42]), and Horoz granitoid (data taken from [38])

Element	Tyana granite Column samples		Horoz granitoid		Üçkapılı granitoid average
			granodiorite average	granite average	
Na_2O%	3.41	3.58	3.85	3.72	3.27
MgO%	2.84	2.81	1.97	1.04	0.47
Al_2O_3%	13.85	13.82	17.77	15,05	13.59
SiO_2%	63.8	64.8	64.36	71.06	73.52
P_2O_5%	0.37	0.36	0.13	0.13	0.04
K_2O%	4.73	4.7	3.68	3.53	2.78
CaO%	3.71	3.63	3.05	1.77	1.99
TiO_2%	0.49	0.46	0.29	0.22	0.21
MnO%	0.11	0.1	0.07	0.03	0.04
Fe_2O_3%	4.04	4.01	3.88	2.47	2.45
LOI	0.64	0.92	0.72	0.82	0.8
Co (ppm)	17.48	17.3	27.51	27.28	9.46
Zn (ppm)	42.54	42.3	25.22	22.04	57.66
Ga (ppm)	18.35	18.35	15.2	14.78	18.46
Rb (ppm)	209.43	210.3	109	98.1	95.63
Sr (ppm)	858.66	859.1	353.59	385.22	385.23
Y (ppm)	46.14	45.2	18.42	13.19	47.23
Zr (ppm)	229.57	230.3	187.31	152.32	151.2
Nb (ppm)	0.91	0.91	17.72	17.63	15.43
Ba (ppm)	1062.63	1064.2	431.25	477.99	395.53
Hf (ppm)	8.98	8.98	3.71	3.28	4.7
Pb (ppm)	47.79	47.6	0.66	4.2	2.46
Th (ppm)	22.45	22.45	11.65	27	9.2
U (ppm)	13.9	13.9	3.49	6	2.1

According to the total alkali (Na_2O + K_2O)-silica (SiO_2) classification diagram [43], the Tyana granite columns and the Horoz Granodiorite samples are located in the granodiorite field, while the Üçkapılı Granitoid and the Horoz Granite samples are located in the granite field (Figure 6a). According to [44], all the rock groups show calc-alkaline features used to distinguish sub-alkaline rocks (Figure 6b). According to the (Na_2O + K_2O) - SiO_2 (wt.%) diagram, the granite columns lie within the alkali granite field [43] (Figure 6a). In the Ab-An-Or classification diagram, Tyana granite columns and Horoz and Üçkapılı granodiorite samples are located in the granodiorite area. The granite samples of Horoz granotoid were observed in the granite field. (Figure 6c). While the average K_2O/Na_2O ratio of the studied granite columns is 1.27, the value of this ratio is 0,85 for the Üçkapılı Granitoid and 0,95 for the Horoz Granitoid. These ratios indicate that all three granitic rocks are K-series igneous rocks [45]. In the Q-P classification diagram based on the cationic ratio of quartz, K-feldspar, and plagioclase [46], the studied columns are classified as granite (Figure 6d). Overall, considering the classification diagrams as a whole, the Tyana granite columns exhibit more similarity to the Horoz Granitoid samples.

The Harker diagrams against SiO_2 for Tyana granite columns and other granitoid samples were drawn and the chemical changes of elements against SiO_2 were analyzed (Figure 7). The changes of the elements in the Harker diagrams of all the rock groups generally show non-regular chemical variations; however, the Tyana granite columns exhibit chemical behavior overall more consistent with the Horoz Granitoid in the studied samples. All the granitoid samples show general negative correlation trends for MgO, FeO_{tot}, TiO_2, and CaO and positive correlation trends for Na_2O and K_2O.

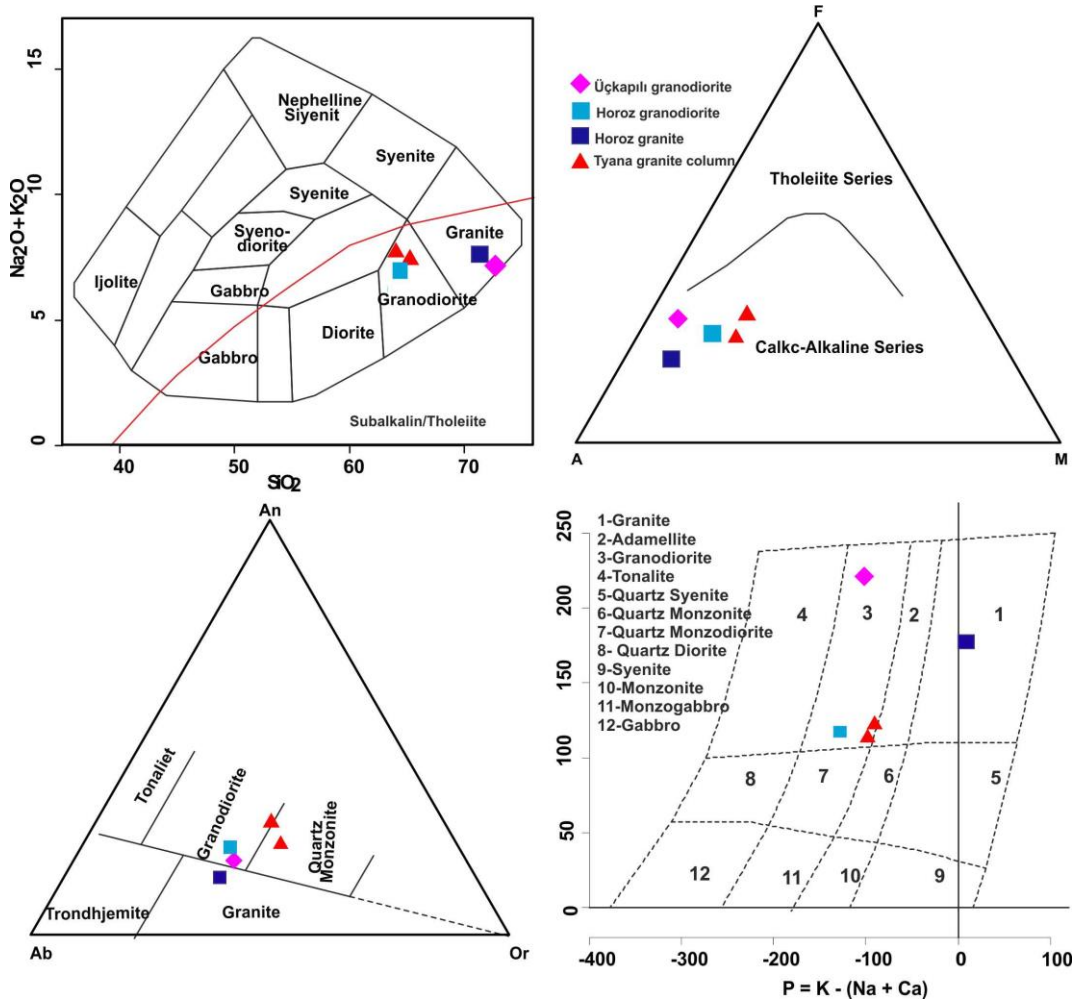

Figure 6. Tyana granite columns and other granitoid samples, a)($Na_2O + K_2O$) (wt.%) vs. SiO_2 (wt.%) diagram [43] b) AFM diagram [44] c) normative Ab-An-Or diagram (O'Connor (1965) d) Q-P diagram [46]

The slightly negative correlations of MgO_t, FeO_{ttot}, TiO_2, and CaO_2 to SiO_2 can be interpreted as a result of the separation of these elements from the igneous system during fractional crystallization. In particular, the decrease of MgO and FeO_{tot} is associated with the crystallization of mafic minerals (e.g., biotite, amphibole, and pyroxene).

In contrast, the positive correlation of Na_2O and K_2O against SiO_2 indicates the crystallization of alkaline bearing phases such as plagioclase and K-feldspar. These chemical variations observed in the Harker diagrams support the interpretation that the Tyana granite columns and the Horoz Granitoid underwent similar magmatic evolutionary processes and that both rocks belong to the calc-alkaline series. In this context, the Tyana granite columns exhibit a magmatic development process more consistent with the Horoz Granitoid than that of the Üçkapılı Granitoid. In general, in all the granitoid samples, a decrease in MgO, FeO_{tot}, TiO_2, and CaO content is observed with weathering of mafic minerals in the early crystallization periods, while the Na_2O and K_2O values increase with late-stage crystallization of alkaline minerals.

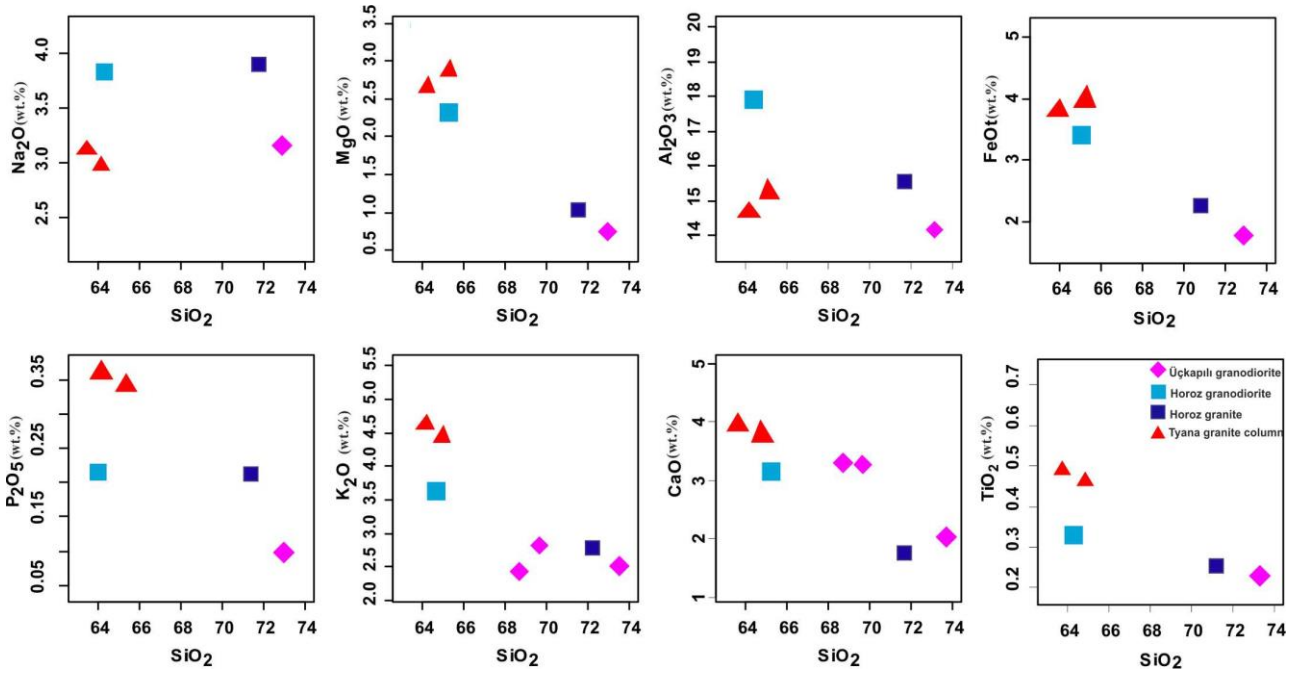

Figure 7. Major oxide Harker diagrams of all granitoid samples

[48] suggested a tectonic classification of granitic rocks based on discrimination diagrams using the elements Rb, Y, Nb, and Ta. In the Rb–(Y + Nb) diagram, which distinguishes between collisional granitoids (syn-COLG), volcanic arc granitoids (VAG), within-plate granitoids (WPG), and ocean ridge granitoids (ORG), the column samples plot within the VAG area (Figure 8a).

In the Nb–Y diagram, both the Tyana granite columns and the Horoz and Üçkapılı granitoid samples plot within the volcanic arc granitoids (VAG/syn-COLG) domain (Figure 8b). The multi-cation R1 and R2 diagram proposed by Batchelor & Bowden (1985) is another widely used classification diagram used to describe the geotectonic environments in which acidic rocks were formed. In these diagrams, the Tyana granite columns and Üçkapılı Granitoid lie within the pre-plate collision area, while the Horoz Granitoid broadly plots within the post-collisional uplift and orogenic fields (Figure 8c).

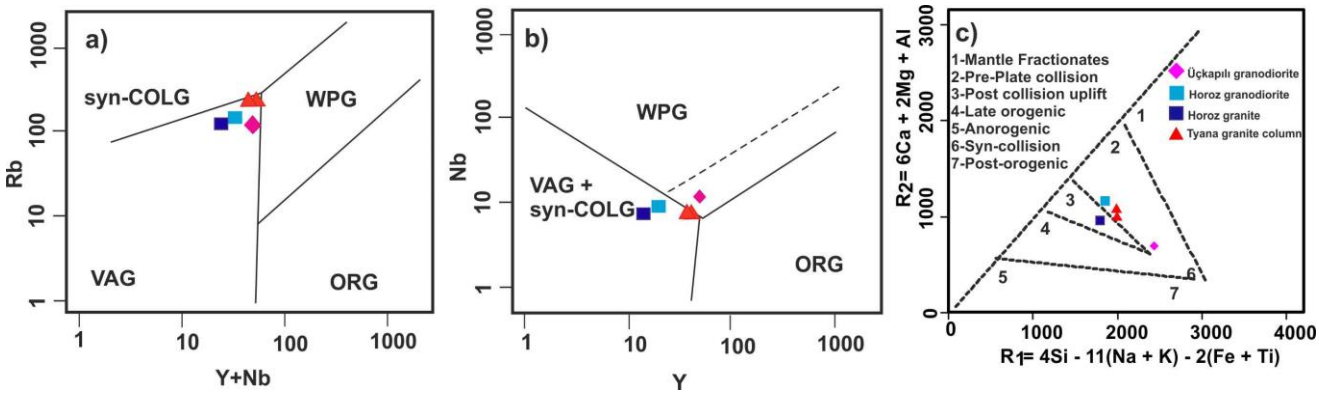

Figure 8. a) Nb -Y tectonic separation diagram [48] b) Rb - (Y + Nb) tectonic separation diagram [48] c) Multi-cation R1-. R2 diagram [49]

6. Conclusion

In this study, the mineralogical, petrographic, and geochemical properties of Tyana granite columns were determined, and petrographic and geochemical analyses were applied to determine their possible origin. Some of the geochemical properties of the Tyana granite columns were compared with those of the nearby Horoz and Üçkapılı granitic rocks, which have been widely discussed in previous literature and are similar in appearance to the Tyana granite columns. The findings from these analyses reveal similarities between the Tyana granite columns and the Horoz granitoid. The results of this study can be summarized as follows.

The granite columns of the ancient city of Tyana exhibit a heterogeneous structure consisting of K-feldspar, plagioclase, quartz, and mafic minerals when evaluated mineralogically and petrographically. The presence of the main mineral phases determined by optical microscope analysis is also consistent with XRD analysis. The CRS studies revealed that the plagioclases have an andesine composition, the amphibole minerals have an actinolite composition, and the biotite minerals are ferro-biotite and biotite in composition.

The Roman granite columns have calc-alkaline affinity with granodiorite composition. In addition, the Roman granite column samples plot in the collisional granitoid (syn-COLG) and volcanic arc granitoid fields,

with similar main oxide and trace element contents to those of the Horoz granitoid. The comparison of the geochemical data of the Horoz granitoid and the Tyana granite columns is also consistent with published data.

In conclusion, the mineralogical, petrographic, and chemical analyses of the granite columns in the ancient city of Tyana presented in this work provide valuable information about the origin of these structures. The analyzed features of the Tyana granite columns are an important input for the conservation and restoration of ancient structures in the future.

Acknowledgement

The author wishes to express sincere appreciation to Prof. Dr. Osman DOĞANAY and the Tyana Excavation team for their permission and assistance in accessing the samples. The analytical work carried out by Aksaray University Applied Geology Laboratory, ASÜBTAM Laboratory, and Ankara University Earth Sciences Application and Research Center (YEBİM) is also gratefully acknowledged.

Author contributions

Hacer BİLGİLİOĞLU: Conceptualization, Methodology, Field study, Data curation, Writing-Original draft preparation, Validation, Visualization, Investigation, Writing-Reviewing and Editing.

Conflicts of interest

There is no conflict of interest.

References

1. Guo, X., Zhang, Y., Xu, X., & Dai, S. (2023). Petrographic and geochemical analyses to characterise the source of built historical natural stones — a case study of the volcanic stones from historical quarries and Baoguosi Temple in the city of Ningbo, China. *Built Heritage*, *7*(1). https://doi.org/10.1186/S43238-023-00091-3
2. Akçe, M. A., & Kadıoğlu, Y. K. (2020). Raman Spektroskopisinin İlkeleri ve Mineral Tanımlamalarında Kullanılması. *Nevşehir Bilim ve Teknoloji Dergisi*, *9*(2), 99–115. https://doi.org/10.17100/nevbiltek.778678
3. Šekularac, N., Ristić, N. D., Mijović, D., Cvetković, V., Barišić, S., & Ivanović-Šekularac, J. (2019). The Use of Natural Stone as an Authentic Building Material for the Restoration of Historic Buildings in Order to Test Sustainable Refurbishment: Case Study. *Sustainability 2019, Vol. 11, Page 4009*, *11*(15), 4009. https://doi.org/10.3390/SU11154009
4. Tavares, M. L., Veiga, M. R., & Fragata, A. (2010). Grouting mortars for consolidation of historical renders showing loss of adhesion. *2nd Conference on Historic Mortars - HMC 2010 and RILEM TC 203-RHM final workshop*, 743–752.
5. Kaderli, L., Tarık Öğreten, M., & Hüsrevoğlu, B. G. (2024). Evaluation of current documentation methods: The case of Kültepe Karum Merchant Quarter. *Cultural Heritage and Science-2024*, *5*(2), 113–128. https://doi.org/10.58598/cuhes.1582187
6. Elyasi, S., & Yamacli, R. (2023). Cultural Heritage and Science Architectural sustainability with cultural heritage values. *Cultural Heritage and Science*, *4*(2), 55–61. https://doi.org/10.58598/cuhes.1282179
7. Biçen Çelik, A., Ay, İ., Ergin, Ş., & Dal, M. (2024). Stone deterioratins in Mardin Madrasas: The case of Şehidiye and Kasımiye Madrasas. *Cultural Heritage and Science*, *5*(1), 38–51. https://doi.org/10.58598/cuhes.1441372
8. Bilgilioğlu, H. (2023). Tarihi harç örneklerinin çoklu analitik yöntemler kullanılarak incelenmesi: Tyana Roma Hamamı (Niğde-Kemerhisar) örneği. *Niğde Ömer Halisdemir Üniversitesi Mühendislik Bilimleri Dergisi*, *12*(4), 1157–1167. https://doi.org/10.28948/NGUMUH.1274588
9. Biçer, A. (2023). Research on The Physical Properties of The Building Stones in East Black See Region. *Naturengs*, *4*(2), 1–6. https://doi.org/10.46572/NATURENGS.1312384
10. Stratton, M. (2003). *Industrial Buildings*. (M. Stratton, Ed.). Taylor & Francis. https://doi.org/10.4324/9780203362471
11. De Vecchi, G., Lazzarini, L., Lünel, T., Mignucci, A., & Visonà, D. (2000). The genesis and characterisation of 'Marmor Misium' from Kozak (Turkey), a granite used in antiquity. *Journal of Cultural Heritage*, *1*(2), 145–153. https://doi.org/10.1016/S1296-2074(00)00162-X
12. Finger, F., Dörr, W., Gerdes, A., Gharib, M., & Dawoud, M. (2008). U-Pb zircon ages and geochemical data for the Monumental Granite and other granitoid rocks from Aswan, Egypt: Implications for the geological evolution of the western margin of the Arabian Nubian Shield. *Mineralogy and Petrology*, *93*(3–4), 153–183. https://doi.org/10.1007/S00710-007-0227-Z/METRICS
13. Kelany, A., Negem, M., Tohami, A., & Heldal, T. (2010). Granite quarry survey in the Aswan region , Egypt : shedding new light on ancient quarrying. *QuarryScapes: ancient stone quarry landscapes in the Eastern Mediterranean*, *12*, 87–98.
14. Klemm, D. D., & Klemm, R. (2001). The building stones of ancient Egypt – a gift of its geology. *Journal of African Earth Sciences*, *33*(3–4), 631–642. https://doi.org/10.1016/S0899-5362(01)00085-9
15. Lazzarini, L. (1998). Sul Marmo Misio, uno dei graniti più usati anticamente. *Studi miscellanei : 31, 1998*, 111–117.
16. Lazzarini. (2010). Six coloured types of stone from asia minor used by the romans, and their

specıfic deterioration problems. *Studies in Conservation*, *55*(sup2), 140–146. https://doi.org/10.1179/sic.2010.55.Supplement-2.140
17. Liritzis, I., Sideris, C., Vafiadou, A., & Mitsis, J. (2008). Mineralogical, petrological and radioactivity aspects of some building material from Egyptian Old Kingdom monuments. *Journal of Cultural Heritage*, *9*(1), 1–13. https://doi.org/10.1016/J.CULHER.2007.03.009
18. Peacock, D. P. S., Williams-Thorpe, O., Thorpe, R. S., & Tindle, A. G. (1994). Mons Claudianus and the problem of the 'granito del foro': a geological and geochemical approach. *Antiquity*, *68*(259), 209–230. https://doi.org/10.1017/S0003598X00046536
19. Williams-Thorpe, O., & Thorpe, R. S. (1993). Magnetic susceptibilıty used in non-destructive provenancing of Roman granite columns. *Archaeometry*, *35*(2), 185–195. https://doi.org/10.1111/J.1475-4754.1993.TB01034.X
20. Koralay, T., Deniz, K., Duman, B., & Kadıoğlu, Y. K. (2021). Mineralogical and geochemical characterization and implications for provenance of Roman granite columns in ancient Tripolis (Denizli, Turkey). *Arabian Journal of Geosciences*, *14*(6), 1–23. https://doi.org/10.1007/S12517-021-06744-W/TABLES/11
21. Cirrincione, R., Fiannacca, P., Ortolano, G., Pezzino, A., & Punturo, R. (2013). Granitoid stones from Calabria (Southern Italy): petrographic, geochemical and petrophysical characterization of ancient quarries of Roman Age. *Periodico di Mineralogia*, *82*(1), 41–59. https://doi.org/10.2451/2013PM0003
22. Williams-Thorpe, O., & Potts, P. J. (2002). Geochemical and Magnetic Provenancing of Roman Granite Columns from Andalucía and Extremadura, Spain. *Oxford Journal of Archaeology*, *21*(2), 167–194. https://doi.org/10.1111/1468-0092.00156
23. Doğanay, O., & İşler, B. (2019). Geç Antik Çağdan Günümüze Tyana (Kemerhisar). *Akdeniz Sanat*, *13*, 639–648. Retrieved from https://dergipark.org.tr/tr/pub/akdenizsanat/issue/49183/622197
24. Şener, H. H., Bacak, K., & Doğanay, O. (2023). Tyana Antik Kenti Su Kemerleri ve Roma Havuzu Üzerine Genel Bir Değerlendirme. *Nevşehir Hacı Bektaş Veli University Journal of ISS*, *13*(4), 2477–2498. https://doi.org/10.30783/NEVSOSBILEN.1323267
25. Gürkan, T., & Doğanay, O. (2020). Tyana Roma Hamamı Kazılarında Ortaya Çıkan Sütun Başlık Parçaları. *Karadeniz Uluslararası Bilimsel Dergi*, *1*(48), 327–353. https://doi.org/10.17498/KDENIZ.833275
26. Günözü, H. (2017). Kapadokya Bölgesi Bizans Dönemi Kaya Kiliseler Duvar Resimlerinde Ticari ve Ticari-Olmayan Enjeksiyon Harçlarının Performans Problemleri Üzerine Analitik Bir Değerlendirme. *Art-Sanat Dergisi*, (8), 153–179. Retrieved from https://dergipark.org.tr/tr/pub/iuarts/issue/47866/604036
27. Karataş, L., Alptekin, A., & Yakar, M. (2023). Material analysis for restoration application: a case study of the world's first university Mor Yakup Church in Nusaybin, Mardin. *Heritage Science*, *11*(1), 1–17. https://doi.org/10.1186/S40494-023-00935-2/TABLES/7
28. Berges, D. (2002). Tyana in Kappadokien: Von der hethitischen Residenz zur gräco-römischen Colonia. *Antike Welt*, *33*(2), 177–187.
29. French, D. (1981). *Roman roads and milestones of Asia Minor = Küçük Asya'daki Roma yolları ve miltaşları*. Oxford B.A.R.
30. Magie, D. (2017). *Roman rule in Asia Minor : to the end of the third century after Christ.* Princeton University Press.
31. Ketin, İ. (1969). Tectonic Units of Anatolia. *Bulletın of The Mıneral Research and Exploratıon*. Retrieved January 27, 2024, from https://dergi.mta.gov.tr/article/show/862
32. Göncüoğlu, M. (1986). Geochronological Data from the Southern Part (Niğde Area) of the Central Anatolian Massif. *Bulletin of the Mineral Research and Exploration*, *105–106*(105–106), 92–106. Retrieved from https://dergipark.org.tr/en/pub/bulletinofmre/issue/3925/52241
33. Dirik, K., & Göncüoglu, M. C. (1996). Neotectonic Characteristics of Central Anatolia. *International Geology Review*, *38*(9), 807–817. https://doi.org/10.1080/00206819709465363
34. Toprak, V., & Göncüoglu, M. C. (1993). Tectonic control on the development of the Neogene-Quaternary Central Anatolian Volcanic Province, Turkey. *Geological Journal*, *28*(3–4), 357–369. https://doi.org/10.1002/GJ.3350280314
35. Çalapkulu, F. (1980). Horoz Granodiyoritinin Jeolojik İncelemesi. *Bulletin of the Geological Society of Turkey*, *23*, 59–68.
36. Kocak, K., & Zedef, V. (2016). Interaction of the lithospheric mantle and crustal melts for the generation of the Horoz pluton (Niğde, Turkey): whole-rock geochemical and Sr-Nd-Pb isotopic evidence. *Estonian Journal of Earth Sciences*, *65*, 138–160. https://doi.org/10.3176/earth.2016.14
37. Kocak, K., Zedef, V., & Kansun, G. (2011). Magma mixing/mingling in the Eocene Horoz (Nigde) granitoids, Central southern Turkey: Evidence from mafic microgranular enclaves. *Mineralogy and Petrology*, *103*(1–4), 149–167. https://doi.org/10.1007/S00710-011-0165-7/FIGURES/10
38. Kadioglu, Y. K., & Dilek, Y. (2010). Structure and geochemistry of the adakitic Horoz granitoid, Bolkar Mountains, south-central Turkey, and its tectonomagmatic evolution. *International*

Geology Review, *52*(4–6), 505–535. https://doi.org/10.1080/09507110902954847

39. Korkanç, M. (2018). Characterization of building stones from the ancient Tyana aqueducts, Central Anatolia, Turkey: implications on the factors of deterioration processes. *Bulletin of Engineering Geology and the Environment*, *77*(1), 237–252. https://doi.org/10.1007/S10064-016-0930-2/FIGURES/13
40. Korkanç, M., & Savran, A. (2015). Impact of the surface roughness of stones used in historical buildings on biodeterioration. *Construction and Building Materials*, *80*, 279–294. https://doi.org/10.1016/J.CONBUILDMAT.2015.01.073
41. Güllü, B., & Akşit, A. (2023). Fingerprint of magma mixture in the leucogranites: Spectroscopic and petrochemical approach, Kalebalta-Central Anatolia, Türkiye. *Open Geosciences*, *15*(1). https://doi.org/10.1515/GEO-2022-0548
42. Kurt, H., Koçak, K., Asan, K., & Karakaş, M. (2013). Petrogenesis of the Üçkapılı Granitoid and its Mafic Enclaves in Elmalı Area (Niğde, Central Anatolia, Turkey). *Acta Geologica Sinica - English Edition*, *87*(3), 738–748. https://doi.org/10.1111/1755-6724.12085
43. Cox, K. G., Bell, J. D., & Pankhurst, R. J. (1979). The Interpretation of Igneous Rocks. *The Interpretation of Igneous Rocks*. https://doi.org/10.1007/978-94-017-3373-1
44. Irvine, T. N., & Baragar, W. R. A. (1971). A Guide to the Chemical Classification of the Common Volcanic Rocks. *Canadian Journal of Earth Sciences*, *8*(5), 523–548. https://doi.org/10.1139/e71-055
45. Ishihara, S., Japan, B. C.-B. of the G. S. of, & 2008, U. (2008). Chemical compositions of the Paleogene granitoids of eastern Shimane prefecture, Sanin district, southwest Japan. *Bulletin of the Geological Survey of Japan*, *59*(6), 225–254.
46. Debon, F., & le Fort, P. (1983). A chemical–mineralogical classification of common plutonic rocks and associations. *Earth and Environmental Science Transactions of The Royal Society of Edinburgh*, *73*(3), 135–149. https://doi.org/10.1017/S0263593300010117
47. U.S. Geological Survey. (1965). *Geological Survey Research 1965*. https://doi.org/10.3133/pp525C
48. Pearce, J. A., Harris, N. B. W., & Tindle, A. G. (1984). Trace Element Discrimination Diagrams for the Tectonic Interpretation of Granitic Rocks. *Journal of Petrology*, *25*(4), 956–983. https://doi.org/10.1093/PETROLOGY/25.4.956
49. Batchelor, R. A., & Bowden, P. (1985). Petrogenetic interpretation of granitoid rock series using multicationic parameters. *Chemical Geology*, *48*(1–4), 43–55. https://doi.org/10.1016/0009-2541(85)90034-8